SOLIDIFICATION STRUCTURE AND HEAT TREATMENT BEHAVIOR OF MULTI-ALLOYED WHITE CAST IRON WITH EXTENSIVE MOLYBDENUM CONTENT FOR APPLYING TO HOT WORK ROLLS

Jatupon Opapaiboon and Patama Visuttipitukul
Department of Metallurgical Engineering, Faculty of Engineering, Chulalongkorn University, Bangkok 10330, Thailand

Sudsakorn Inthidech [ORCID]
Department of Manufacturing Engineering, Faculty of Engineering, Mahasarakham University, Mahasarakham 44150, Thailand

Yasuhiro Matsubara
National Institute of Technology-Kurume College, Fukuoka 830-8555, Japan

Abstract

In this work, the effect of Mo content on solidification structure and heat treatment behavior of multi-alloyed white cast iron was investigated. Cast irons with varying Mo content from 0.12 to 7.66 wt% under the other alloying elements with basic composition were prepared. The solidification sequences were investigated by means of thermal analysis methods. After annealing, the specimens were hardened from 1050 °C by liquid nitrogen spray and subsequently tempered at 400–600 °C. It was found that the solidification sequence of all specimens started with primary austenite dendrite (γ_p) and was followed by eutectic reactions. The first eutectic reactions began with $L_1 \rightarrow (\gamma + MC)$ and are followed by $L_2 \rightarrow (\gamma + M_7C_3)$ for specimens with Mo less than 1.17 wt% and $L_2 \rightarrow (\gamma + M_2C)$ for specimens with Mo more than 3.02 wt%, respectively. As Mo content rose, the solidification temperature range of ($\gamma + MC$) eutectic decreased but that of ($\gamma + M_2C$) eutectic increased when the Mo content rose over 3.02 wt%. The area fraction of ($\gamma + MC$) eutectic decreased while ($\gamma + M_2C$) eutectic increased with an increase in Mo content. With respect to heat treatment behavior, hardness in the as-hardened state increased proportionally but volume fraction of retained austenite ($V\gamma$) dropped progressively as Mo content increased. All the tempered hardness curves showed more or less secondary hardening depending on the Mo content. The maximum tempered hardness (H_{Tmax}) was obtained at 525 °C tempering where the $V\gamma$ value was less than 3%. The highest values of H_{Tmax}, 913 HV30 for macro-hardness and 890 HV0.1 for micro-hardness, were obtained, respectively, in the specimen with 4.98 wt%Mo.

Keywords: multi-alloyed white cast iron, solidification sequence, heat treatment, maximum tempered hardness, retained austenite, mo influence

Introduction

Alloyed white cast iron has been widely used for a long time as material for machine parts in mining, cement and steel-making industries[1–3]. The surface of such machine parts is heavily worn by abrasive materials in operations. The development of roll materials started with low-alloyed white cast iron through Ni-hard and high chromium cast irons which are very popular as practical applications[2,3]. Although high Cr cast iron has high abrasive wear resistance[4–7], a large amount of eutectic carbide in the microstructure tends to reduce the toughness of the roll. Therefore, new types of roll materials with much higher performance than Ni-hard and high Cr cast irons have been increasingly demanded.

The finishing hot rolling mill for steel consists of 6 or 7 stands with work rolls which are placed side by side, and the hot steel plate is rolled continuously to reduce the thickness. During rolling operation, the temperature of the roll surface increases up to 500–700 °C depending on the kind of steel and roll in the stand[2]. The temperature of the roll at the first stand is highest and it decreases as the roll moves to the backward stands in sequence. It is because of the contact area between roll and strip decreases and the rotating speed increases. Therefore, the main requirements of a hot work roll are high hardness, high softening resistance and high wear resistance at elevated temperature. In rolling, the heat and slip of steel are basically main factors influencing the wear resistance[2]. From the viewpoint of microstructure of roll materials, the amount and distribution of plural eutectic carbides with high hardness and the strengthened matrix with tempered martensite, secondary carbides and very less retained austenite are very important factors[2,8–10].

Thirty years ago, multi-alloyed white cast iron which contains plural kinds of strong carbide formers such as Cr, Mo, W and V was devised by a Japanese group for this purpose and the development has been continued up to now [3]. The basic alloy composition of the cast iron is 2 wt%C (hereafter wt% is expressed by %), and Cr, Mo, W and V each with 5%[3]. The carbide-forming elements combine with C to form their eutectic carbides with extremely high hardness. Also, residual elements dissolving in the matrix improve the heat treatment behavior and provide a suitable matrix microstructure. V combines with C to form MC carbide during solidification. The eutectic MC carbide contains more than 50%V and crystallizes with nodular or plate-like morphology[11]. The hardness of MC carbide is about 2600–2800 HV. Since the average diameter is in the range of 5–20 μm[10], the MC eutectic carbides can be distinguished clearly by OM and SEM. The MC eutectic carbide is very effective against the abrasive wear resistance of the roll. The nodular morphology of MC eutectic carbide could improve the toughness because of less notch effect[7–10]. The fine MC carbides could precipitate secondarily in the matrix of heat-treated multi-alloyed white cast iron. It is considered that the fine MC carbides precipitate when martensite is tempered by carbide reaction. However, it is hard to distinguish them in SEM microphotographs because the size of precipitated MC carbides is very fine. The MC secondary carbides have extremely high hardness and significantly promote the secondary hardening of the matrix. Cr forms M_7C_3 (1200–1800 HV) and $M_{23}C_6$ (850–1100 HV) carbides. This type of carbide has good abrasive wear resistance and proper toughness due to interconnected morphology[1]. It is well known that Cr improves the hardenability of the cast iron by suppressing the pearlite or bainite transformation. Mo and W are also strong carbide-forming elements and form M_2C (1500–1800 HV) or M_6C (1800–2200 HV) carbide[10,11]. It was reported that Mo tends to stabilize the M_2C carbide

while W tends to form M_6C carbide[10]. Both Mo and W promote the secondary precipitation hardening of the matrix by tempering. Since Mo forms M_2C carbide with high hardness and improves hardenability by postponing pearlite transformation, Mo is one of the most important elements in the basic carbide formers in the multi-alloyed white cast iron. Co is not a carbide forming element but most of Co distributes to matrix where it improves strength at high temperature and improves resistance to softening due to tempering and the coarsening of grain[3].

Currently, multi-alloyed white cast irons have been preferably used for hot work rolls in steel making and recently, attempts were made to apply them to the parts of mineral pulverizing machines. It was reported that the rolling mill rolls made by this kind of cast irons showed higher quality and performance, and the service life was dramatically extended for 3–5 times as long as the conventional rolls made of Ni-hard and high Cr cast irons[8]. Unquestionably, the application of multi-alloyed white cast iron will be expanded increasingly to various industrial fields in the near future. From these viewpoints, it is considered that the research of this type of cast iron on solidification structure and heat treatment behavior is very significant and helpful for developing more practical applications.

For roll materials, the amount of retained austenite in the matrix is one of the important factors to which should be given attention. The retained austenite must be kept at low value because it lowers hardness and causes a change in dimensions of roll due to the transformation. Furthermore, the retained austenite may lead to cracking during service because of the volume expansion by the stress-induced martensite transformation[2]. Therefore, heat treatment is generally given to the cast irons to control the amount of retained austenite and to improve the mechanical properties as well as the wear resistance.

Heat treatment processes of multi-alloyed white cast iron are carried out in the same manner as tool steel and high Cr cast iron, i.e., annealing, hardening and tempering. It is characteristic in alloyed white cast iron that the austenite is destabilized by precipitating secondary carbides during austenitizing, and then it transforms to martensite by quenching. However, some austenite is usually retained after quenching because a high concentration of alloying elements dissolved in austenitized matrix causes Ms temperature to decrease. In tempering, the secondary carbides can precipitate in the residual austenite after hardening and allow its martensite transformation during post-cooling. Besides, the special carbides with extremely high hardness could precipitate secondarily from martensite at a certain tempering temperature by the so-called carbide reaction.

The role of Mo in the heat treatment behavior of the multi-alloyed white cast irons hardened from 1100 °C was

reported in previous work[12]. In that work, the hardness was improved by Mo addition but quite a lot of austenite still remained after tempering even in the specimens with maximum tempered hardness (H_{Tmax}). This was because higher austenitizing temperature makes the austenite more stable. Therefore, to reduce the final amount of retained austenite, a lower austenitizing temperature than 1100 °C has to be selected when hardening. On the hot work roll with a large section, the high austenitizing temperatures of 1050–1100 °C are recommended. Low austenitizing temperature should be insufficient for homogenization of austenite as well as for inadequate dissolution of secondary carbides formed by annealing, and that affects the final quality of rolls in respect of hardness and wear resistance.

The solidification sequence[10], heat treatment[12–18] and wear behaviors[18,19] of multi-alloyed white cast irons with basic alloy composition have already been reported by our group. However, systematic research on solidification structure and heat treatment behavior of multi-alloyed white cast irons with extensive Mo content has not been reported. In this work, therefore, the effect of Mo content on solidification structure or microstructure feature and heat treatment behavior in which the austenitizing temperature was lower of 1050 °C compared with 1100 °C in the previous work[12] was investigated.

Experimental Procedures

Preparation of Specimens

Test specimens were prepared with the same methods as previous works[12]. The shape and dimensions of the CO_2 bonded sand mold to make the test ingot is shown in Figure 1. The cavity size of the mold was φ2.5 x 6.5 cm and with sufficient top riser. The charge materials with target chemical composition were melted in an induction furnace with alumina lining. Since the multi-alloyed white cast iron contains alloying elements of Mo, W, V with very high melting points, it is necessary to make the melt homogeneous in such alloying elements and pour it at higher temperature without any crystallization of carbides with such strong carbide formers before pouring. After superheating the melt to 1580 °C, the melt was held for 10 min and then, poured into a preheated mold at 1500–1520 °C. The riser was instantaneously covered with dry exothermic powder. The chemical compositions of test specimens are shown in Table 1.

Thermal Analysis

To investigate the solidification sequence, thermal analysis testing was carried out for each specimen. The equipment is illustrated in Figure 2. Sample (55g) was re-melted in an alumina crucible using an electric furnace with SiC
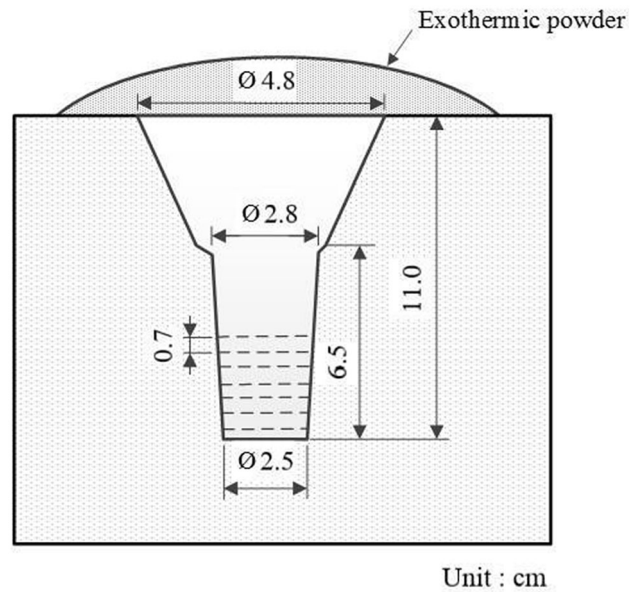

Figure 1. Schematic drawing of sand mold to make test ingots.

Table 1. Chemical Composition of Test Specimens.

Specimen	Elements (wt%)					
	C	Cr	Mo	W	V	Co
No. 1	2.05	5.13	0.12	4.95	5.09	1.99
No. 2	2.08	5.09	1.17	4.92	5.03	2.01
No. 3	2.09	5.11	3.02	5.06	5.10	2.01
No. 4	2.00	4.96	4.98	4.98	5.01	2.03
No. 5	2.06	5.00	7.66	4.98	5.01	1.98

① Automatic Recorder
② R thermocouple
③ Argon gas inlet tube
④ Alumina tube
⑤ Alumina crucible
⑥ Graphite rod
⑦ Silicon carbide resistance furnace
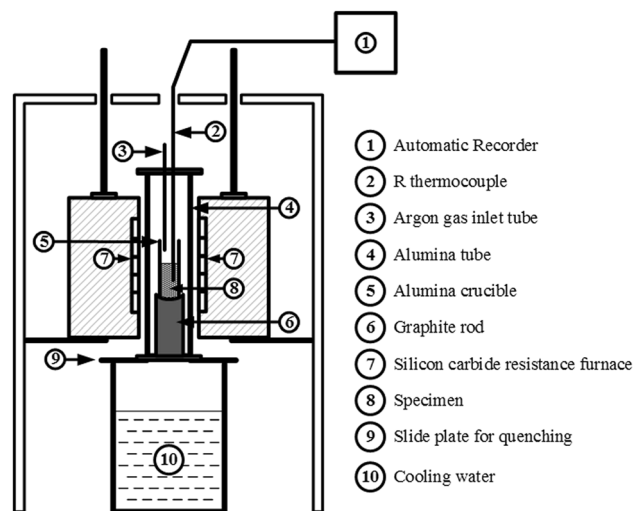⑧ Specimen
⑨ Slide plate for quenching
⑩ Cooling water

Figure 2. Schematic drawing of equipment for thermal analysis test.

resistance under Ar atmosphere. The melt was heated up to 1500 °C and held there for 15 min. After holding, the melt was cooled down to 950 °C at approximately 0.3 °C/s. An AR-type thermocouple was submerged into the melt and a cooling curve was obtained by an automatic Y-T recorder.

Heat Treatment Process

Test ingots were coated with an anti-oxidation paste to prevent the test pieces from oxidation and decarburization during heat treatment. For annealing, the ingots were heated to 950 °C in an electric furnace. After holding at the temperature for 5 h, the ingots were cooled in the furnace (FC). Annealed ingots were cut by a wire-cutting EDM machine to obtain a test piece 0.7 cm in thickness. The test pieces were austenitized all together at 1050 °C for 1 h in a vacuum furnace and then quenched by liquid nitrogen spray (LNS). Hardened test pieces were tempered at 400-600 °C with 50 °C intervals in an electric furnace. After holding for 200 min, the test pieces were cooled to room temperature in air (AC).

Microstructure Observation

Total microstructure of each specimen was observed by an optical microscope (OM). The test pieces were polished using emery papers and buffing. Nital and Murakami's reagents were adopted to identify the type of eutectic carbide and Villella's reagent was introduced to reveal the matrix microstructure. The matrix microstructure was observed by scanning electron microscope (SEM) and microphotographs were taken focusing on the dendrite areas for discussions.

Measurement of Hardness and Volume Fraction of Retained Austenite (Vγ)

Macro-hardness or total hardness of specimens was measured by a Vickers hardness tester with a load of 30 kgf. Micro-hardness or matrix hardness was performed in the primary austenite region by Micro-Vickers hardness tester with a load of 100 gf. In each specimen, the hardness was randomly measured at five points and the average value was adopted.

Volume fraction of retained austenite (Vγ) was measured using an X-ray diffraction method. A special simultaneously rotating and swinging sample stage was used to cancel the preferential crystal orientation effect of austenite[20]. The X-ray beam source was Mo-K$_\alpha$ passed through a Zr filter. The scanning range was from 24 to 44 degrees by 2θ. The diffraction peaks adopted for quantitative calculation of austenite were (200) and (220) planes for ferrite and/or martensite and (220) and (311) planes for austenite. The Vγ was calculated by the integrated area under the selected peaks using an image analysis software. Further details on measurement of Vγ were reported by the references[12–19].

Results and Discussions

### Effect of Mo Content on Solidification Structure

The mirror-polished as-cast specimens were etched by Nital etchant first and followed by Murakami's reagent, and their microphotographs are representatively shown in Figure 3. It was found that all the specimens had hypoeutectic composition which consisted primary austenite dendrite (γ_p) and eutectic structure (γ+carbide). It was found that the eutectic carbides within these alloy compositions were MC and M_2C or M_7C_3 types depending on the Mo content. The morphology of MC carbide was string-like or coral-like and that of M_2C carbide was lamellar or plate-like while the M_7C_3 carbide had rod-like or ledeburitic morphology[10,11]. Furthermore, these carbides could be identified by Murakami's reagent, that is, the M_2C and M_7C_3 carbides turn brown but the MC carbide does not. It was found that the eutectic carbides in the specimens with less than 1.17%Mo were MC and M_7C_3 types and those in the specimens with Mo content of more than 3.02% were MC and M_2C types. This is because an increase in the Mo content over 3.02% can inhibit the formation of M_7C_3 carbide and instead, Mo promotes the crystallization of M_2C carbide.

From the observation of as-cast microstructure, it is found that (γ+M_2C) eutectic begins to crystallize in the specimen with Mo of more than 3.02%. In order to clarify the solidification sequence, therefore, thermal analysis tests were carried out for the specimens of No. 3 (3.02%Mo), No. 4 (4.98%Mo) and No. 5 (7.66%Mo). The cooling curve of specimens with highest Mo content of 7.66% is representatively shown in Figure 4. The first derivative graph (dT/dt) of the specimen is displayed in red in the same figure. The solidification started with crystallization of primary austenite (γ_p), followed by eutectic reaction of L→(γ+MC) and the solidification ended with that of L→(γ+M_2C). The results agree well with those by Wu et al[11]. To determine the temperature of each solidification which appears as a recalescence, the peaks of the first deviation graph of the cooling curve, which was made by adopting about 1200 points of data on the thermal analysis curve, was compared with the cooling curve and the freezing point for each reaction was determined. The first peak appearing at highest temperature should be the
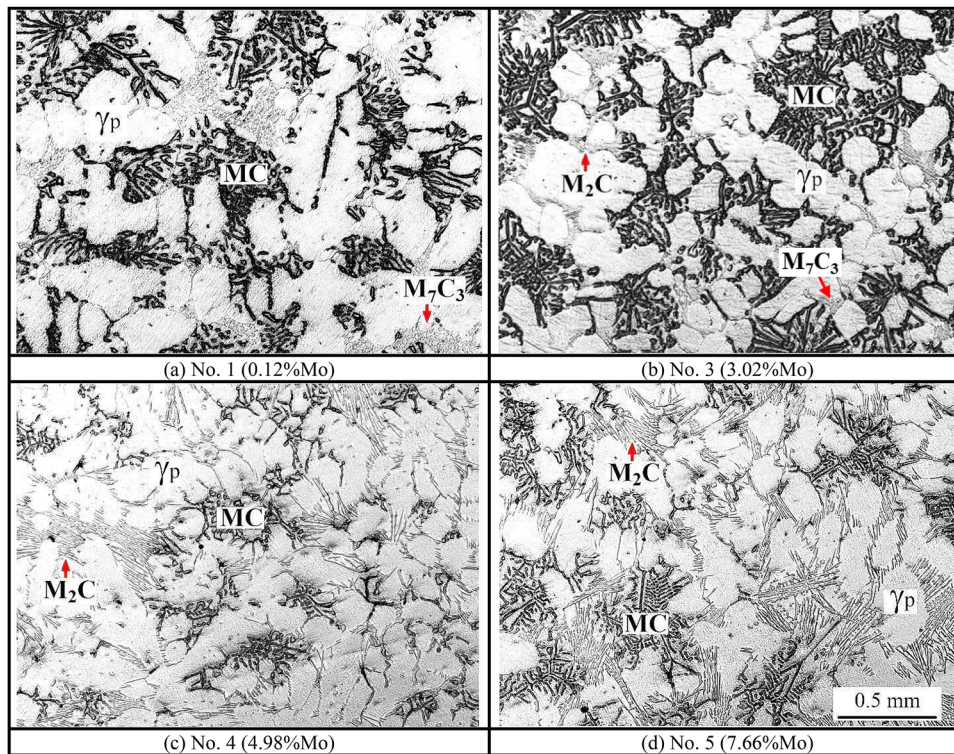
Figure 3. Optical microphotographs of as-cast specimens with different Mo contents.
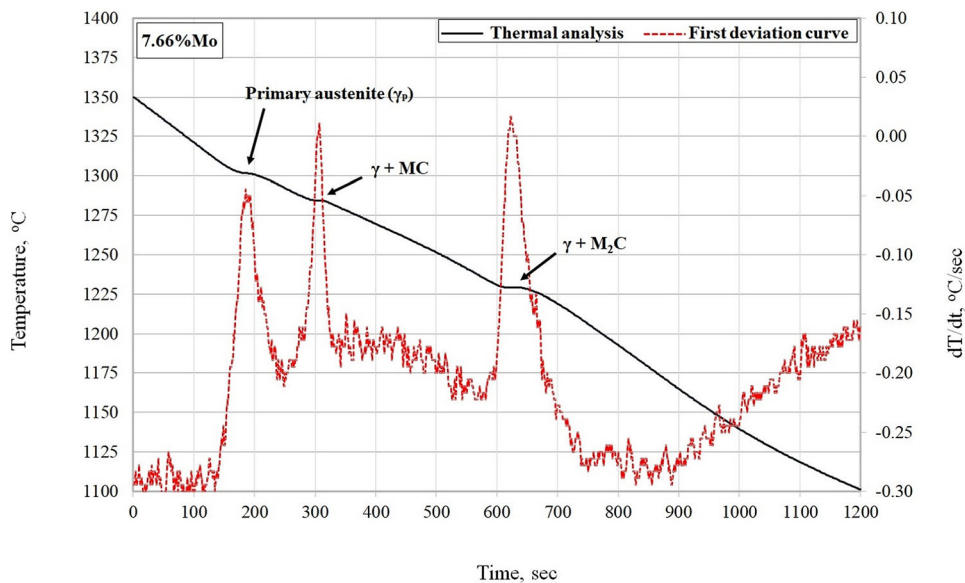
Figure 4. Comparison of thermal analysis curve and first deviation graph of specimen (No. 5) with 7.66%Mo.

crystallization of γ_p followed by the (γ+MC) eutectic and (γ+M_2C) eutectic reactions, respectively.

The thermal analysis curves of specimens with 3.02%, 4.98% and 7.66%Mo are shown in Figure 5. The start temperatures of three solidification reactions in the specimens with 3.02 and 4.98%Mo are similar but that of γ_p crystallization in the specimen with 7.66%Mo is lower than the other two specimens. The solidification sequences and the start temperature of each reaction in the specimens with 3.02%, 4.98% and 7.66%Mo are summarized in Table 2.

To clarify the effect of Mo content on the solidification sequences summarized in Table 2, the relationship between start of solidifying temperature for primary austenite (γ_p), (γ+MC) and (γ+M_2C) eutectic reactions and Mo content
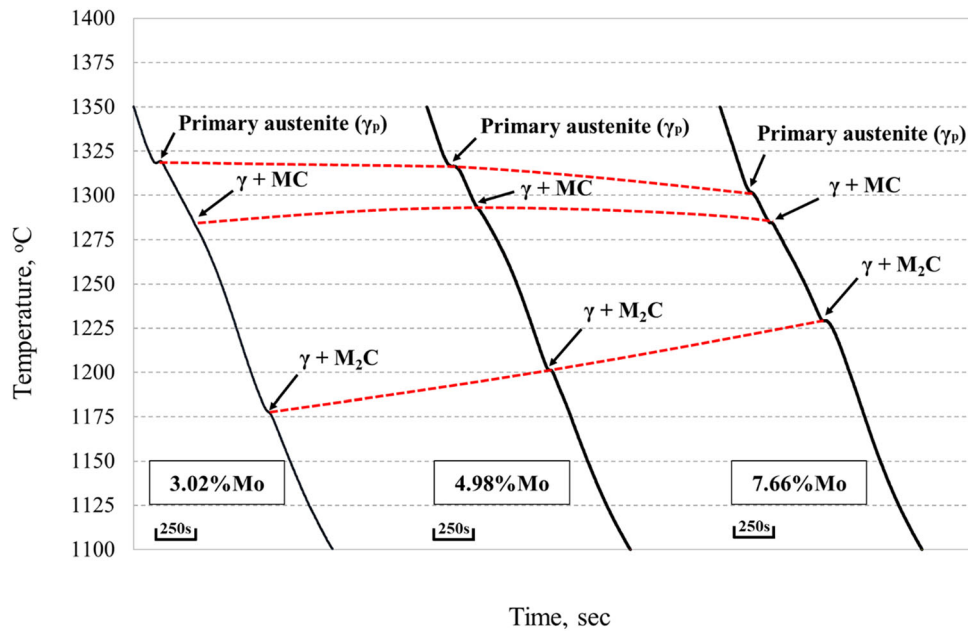
Figure 5. Thermal analysis curves of specimens with different Mo content.

Table 2. Solidification Sequences and Beginning Temperature of Solidification of Specimens Different Mo Contents.

Specimen	Solidification reaction and start temperature	
No. 3	$L_0 \rightarrow \gamma_p + L_1$	at 1319°C
(3.02%Mo)	$L_1 \rightarrow (\gamma + MC) + L_2$	at 1284°C
	$L_2 \rightarrow (\gamma + M_2C)$	at 1177°C
No. 4	$L_0 \rightarrow \gamma_p + L_1$	at 1316°C
(4.98%Mo)	$L_1 \rightarrow (\gamma + MC) + L_2$	at 1292°C
	$L_2 \rightarrow (\gamma + M_2C)$	at 1200°C
No. 5	$L_0 \rightarrow \gamma_p + L_1$	at 1301°C
(7.66%Mo)	$L_1 \rightarrow (\gamma + MC) + L_2$	at 1284°C
	$L_2 \rightarrow (\gamma + M_2C)$	at 1229°C

Figure 6. Effect of Mo content on start temperatures of each solidification reactions, primary austenite (γ_p), ($\gamma+MC$) and ($\gamma+M_2C$) eutectics.

is graphically shown in Figure 6. The start of solidification temperatures of γ_p decreased slowly from 1319 to 1301 °C but that of ($\gamma+MC$) eutectic changed little as the Mo content increased. However, the start temperature of ($\gamma+M_2C$) eutectic solidification increased clearly from 1177 to 1229 °C with an increase in Mo content. This is because higher Mo combines with more C to form ($\gamma+M_2C$) eutectic and then, the liquidus temperature of ($\gamma+M_2C$) eutectic solidification increased due to the reduction of C content. From these results, it became clear that the solidification temperature range of this system alloy decreases clearly with increasing Mo content.

To confirm the solidification sequence shown in Table 2, a quasi-binary phase diagram of M (Fe-5%Cr -5%W-5%V-2%Co)-Mo-2%C system was obtained using THERMO-
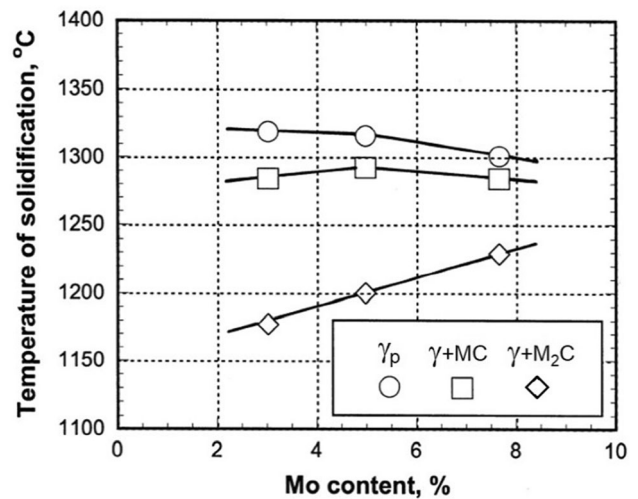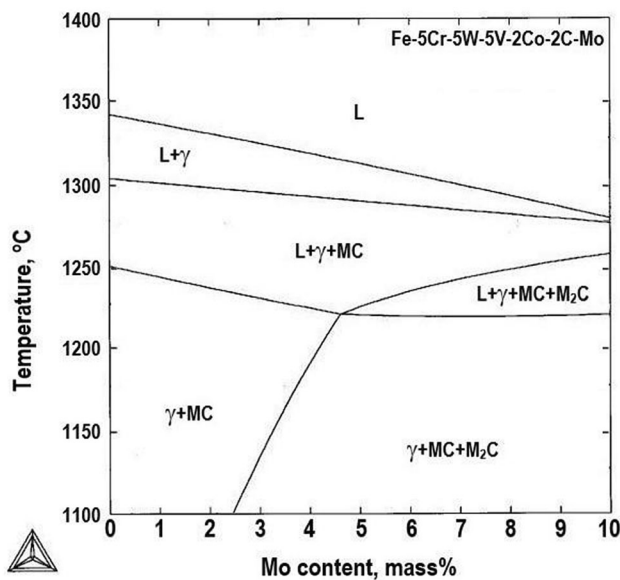
CALC software and the result is shown in Figure 7. It was found that the contours of the solidification temperatures of primary austenite (γ_p) and two kinds of eutectics were similar to the experimental results summarized in Figure 6. However, there were some differences in the freezing temperature of each eutectic reaction. Particularly, the Mo content at ($\gamma+M_2C$) eutectic point was higher than that obtained by the experiment. This was because the prediction by THERMO-CALC was under the equilibrium condition, i.e., the supercooling of the melt or the segregation of alloying elements during solidification was not taken into account. Nevertheless, it is convincing that the diagram in Figure 7 is close to the results obtained by the experiment. As for the diagram in Figure 7, the

Figure 7. Quasi-binary phase diagram of M (Fe-5%Cr-5%W-5%V-2%Co)-Mo-2%C alloy by THERMO-CALC software.

Figure 8. Effect of Mo content on area fraction of primary austenite dendrite (γ_p) and eutectic structures in the as-cast specimens.

solidification starts with crystallization of γ_p and is followed by (γ+MC) eutectic reaction up to 10%Mo. The (γ+M$_2$C) eutectic appears above 4.5%Mo. The beginning temperatures of γ_p and (γ+MC) eutectic solidifications decrease progressively but that of (γ+M$_2$C) eutectic increases gradually as the Mo content rises over 4.5%Mo. Furthermore, the finishing temperature of solidification for (γ+M$_2$C) eutectic changes little even if the Mo content is varied. Therefore, the solidification temperature range of γ_p and (γ+M$_2$C) eutectic decreases but that of (γ+M$_2$C) eutectic increases with a rise of Mo content. From the comparison of the results from the experiment with those from THERMO-CALC, it can be said that the solidification sequence clarified by the experiment is reasonable.

It is profitable for alloy design engineers to know the amount of constituent phases in the microstructure changes resulting from addition of Mo. The area fraction or the amount of each phase in the as-cast microstructure was measured using an image analyzer and the result is shown in Figure 8. The amount of primary austenite (γ_p) did not change much even if Mo content increased through a wide range. However, the amount of eutectic structures varied greatly depending on the Mo content. The (γ+M$_7$C$_3$) eutectic which existed already in low Mo specimens, decreased slightly with an increase in Mo content and at around 1.17%Mo, it did not appear anymore. Instead, the (γ+M$_2$C) eutectic appeared at 3.02%Mo and increased in proportion to the Mo content. With respect to (γ+MC) eutectic structure, the amount decreased progressively over 3.02%Mo. These results were in good accordance with those of thermal analysis tests shown in Figure 5; that is, the solidification temperature range of (γ+MC) eutectic
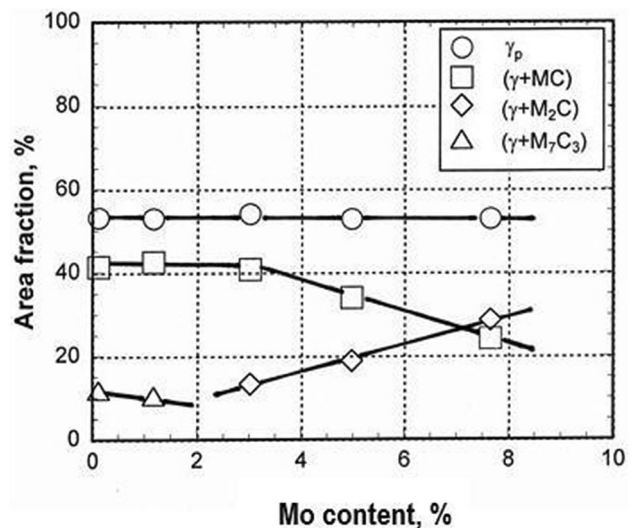
became narrow due to an increase in that of (γ+M$_2$C) eutectic.

Effect of Mo Content on Heat Treatment Behavior

As-Hardened State

As mentioned before, heat treatment must be given to the alloyed white cast irons to improve the mechanical properties and wear resistance. Although the morphology of eutectic carbides changes little by heat treatment because of their high thermal stability[10], the matrix varies greatly subject to not only heat treatment condition, but also kind and amount of alloying elements. SEM microphotographs focusing on the matrix region in the as-hardened specimens are shown in Figure 9. The matrices of all the specimens were made up of martensite (M), secondary carbide (Cs) and retained austenite (γ_R). The fine carbides were observed throughout the matrix. It is evident that carbides existed already in the austenitized matrix and the residual austenite filling the gap among carbides transformed to martensite by quenching. These carbides could first precipitate secondarily during annealing and a large portion of them remained without dissolving into austenite in spite of heating up for austenitization. The martensite in the matrix cannot be distinguished clearly in these microphotographs but it is presumed from the matrix hardness (873HV0.1 to 946HV0.1) that the martensite exists in the matrix. The secondary carbides could be MC, M$_6$C and M$_7$C$_3$ types as reported by Hashimoto et al[21]. It seems that the precipitated carbides increased in number with a rise in Mo content. The reasons can be explained as follows.
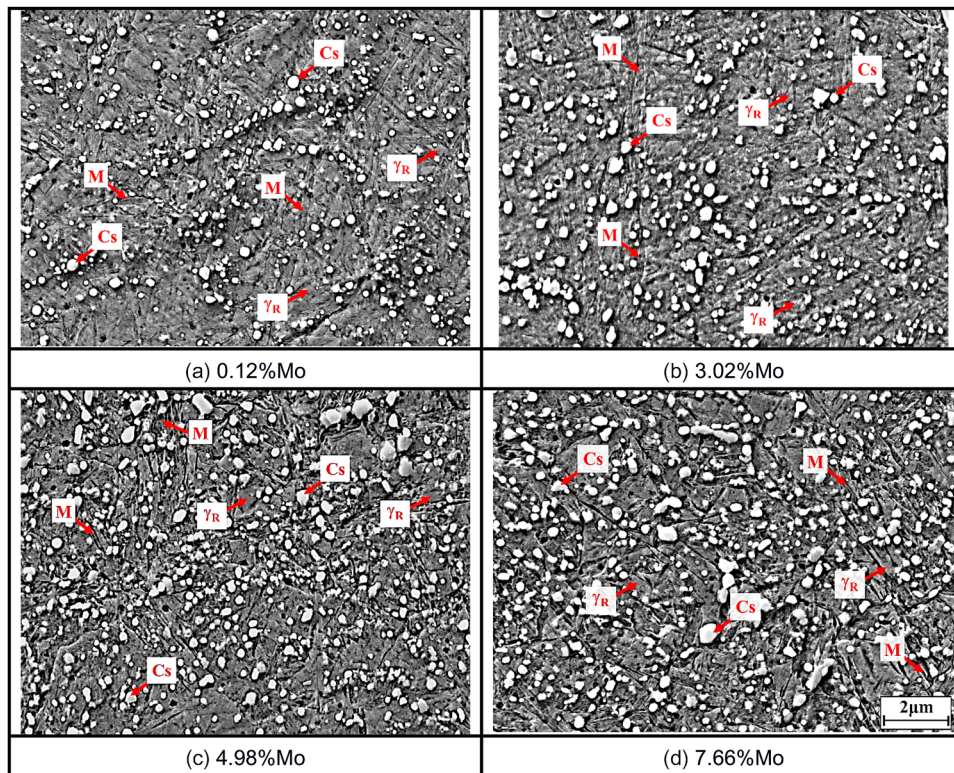
Figure 9. Matrix microstructures of as-hardened specimens with different Mo contents. Austenitizing: 1050 °C. (γ_R: Retained austenite, M: Martensite, Cs: Secondary carbide).

It is known that the precipitation rate of secondary carbide is controlled by the diffusion rate of the carbide formers and carbon. Since Mo is one of the strong carbide formers and it has high ability to form carbide even at high temperature, an increase in Mo content causes more Mo to dissolve in austenite and promotes the precipitation of total secondary carbides. Consequently, a large number of secondary carbides could precipitate in specimens with high Mo content. Compared with the previous work[12] in which the specimens were austenitized at 1100 °C, the secondary carbides in this experiment were in greater amount. It can be understood that the solubility of C and other alloying elements in austenite is increased when the austenitizing temperature is elevated. The higher austenitizing temperature promotes carbon and other alloying elements to better dissolve in austenite and restrains the driving force to precipitate the secondary carbides.

The effect of Mo content on macro-hardness, micro-hardness and Vγ in the as-hardened state is shown in Figure 10. The data obtained in the previous work[12] were added in the diagram for comparison. It was found that the macro-hardness and micro-hardness showed the same behavior, i.e., both increased proportionally to the Mo content. This was because the amount of hard eutectic M_2C carbides, secondary carbides and martensite increased. By contrast, the Vγ value decreased gradually as the Mo content rose. It can be explained that an increase in the amount of
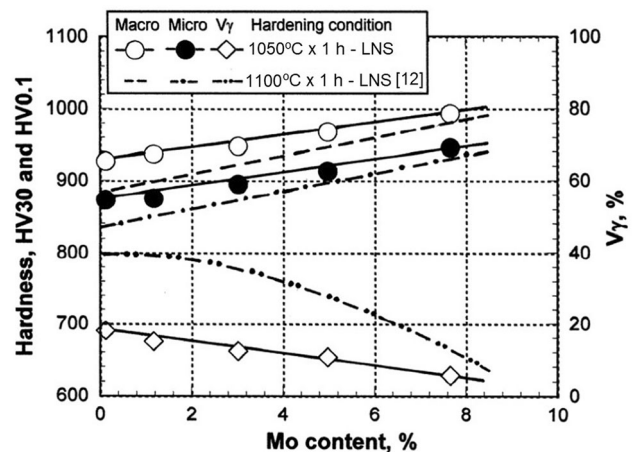
Figure 10. Effect of Mo content on macro-hardness, micro-hardness and volume fraction of retained austenite (Vγ) in the as-hardened state. Austenitizing: 1050 °C. (line: Austenitizing: 1100 °C[12]).

precipitated carbides with rising Mo content as previously mentioned, reduced the amount of C and alloying elements in austenite and hence, the Ms temperature was increased.

It is clear in Figure 10 that the quenched hardness in this experiment was higher, but that of the Vγ value was lower than those reported in the previous work. It is considered that the increase of hardness in this experiment was caused

by two factors; an increase in the precipitation of secondary carbides and an increase in the amount of martensite. The latter reason results from the concentration of C and alloying elements dissolving in the austenite at lower austenitizing temperature being low and Ms temperature was high.

As mentioned before, the eutectic carbides changed very little by heat treatment and therefore, the variation of macro-hardness was mainly influenced by matrix hardness or micro-hardness. The relationship between micro-hardness and Vγ value of as-hardened specimens is shown in Figure 11. The micro-hardness lowers nearly proportionally as the Vγ value increased. It is natural that an increase of retained austenite in the matrix and a decrease in both the martensite and precipitated carbides caused the matrix hardness to decrease.

Tempered State

The relationships between macro-hardness, micro-hardness, Vγ and tempering temperature of all the specimens are shown in Figure 12. The micro-hardness showed a similar trend to that of the macro-hardness. However, the micro-hardness is located at a lower position than the macro-hardness. This is because macro-hardness is the sum of the eutectic carbides and matrix. The tempered hardness curves involved more or less the secondary hardening as shown by the graphs. At the lowest tempering temperature of 400 °C, the hardness dropped largely from that in an as-hardened state because the high hardness caused by lattice strain in martensite was relieved. As the tempering temperature was elevated, the tempering of martensite continued and the hardness also decreased. When the temperature approached 500 °C, the so-called carbide reaction starts[22, 23], and there, nearly pure carbides such as
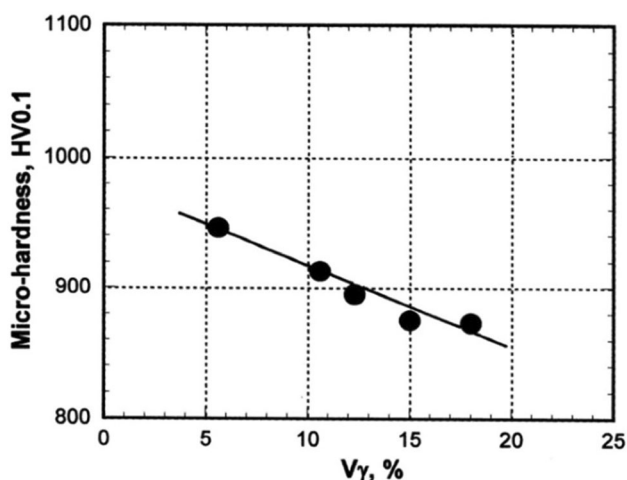
VC and $(Mo,W)_2C$ precipitate from M-type carbides like MC and M_2C[23]. However, the retained austenite is decomposed or destabilized by the precipitation of secondary carbides and it causes the Ms temperature to rise. Resultantly, residual retained austenite transforms to martensite during post cooling. In the case where both situations have occurred, the total hardness reaches the maximum value of tempered hardness (H_{Tmax}) which was obtained by tempering at 525 °C in all specimens. When the tempering temperature rises above 525 °C, however, the agglomeration of secondary carbides occurs due to the Ostwald ripening effect. Then, the hardness drops remarkably. The degree of secondary hardening, which is defined by the difference between the hardness at which secondary hardening begins and the H_{Tmax}, was high in all the specimens except for 7.66%Mo. It is considered that the secondary hardening could be involved with the Vγ value in an as-hardened state.

As shown by the Vγ graphs in Figure 12, the Vγ value of each specimen decreases steeply as the temperature increased from 450 to 525 °C and the tendency corresponds to the trend of secondary hardening in inverse proportion. This indicates that the decomposition rate of retained austenite is high in the temperature range from 450 to 525 °C, in other words, the precipitation of secondary carbides is active and a great deal of austenite was decomposed or destabilized to encourage the martensite transformation during post cooling. When the tempering temperature rises over 525 °C, the Vγ value is lowered to quite a low level. At 600 °C tempering, the matrix becomes carbide and ferrite and the Vγ value is almost nil. The Vγ value at H_{Tmax} was less than 3% in all specimens.

To confirm the experimental results obtained, the matrix microstructures of as-hardened specimens with 4.98%Mo and those of tempered specimens at different temperatures were observed by SEM. The SEM microphotographs are displayed in Figure 13. In the as-hardened specimen (a), more austenite is recognized coexisting with martensite in the gap of secondary carbides. It is considered that much of the larger secondary carbides could have precipitated previously in the annealing process and they were left indissoluble during austenitizing. In the matrix of specimens tempered at 450 °C (b), the amount of retained austenite decreases from that of the as-hardened specimen. Additionally, the newly precipitated fine carbides were observed. In the specimen tempered at 525 °C (c), where the H_{Tmax} was obtained, much more fine carbides existed. These carbides should be in the state just before the carbides begin to coarsen. In this state, the matrix should be a tempered martensite. In the tempering at 600 °C (d),

Figure 11. Relationship between micro-hardness and volume fraction of retained austenite (Vγ) in as-hardened state. Austentizing: 1050 °C.

however, there are many of large secondary carbides. In this state, either martensite or residual austenite cannot be present, i.e., so-called over-tempering state. Therefore, the
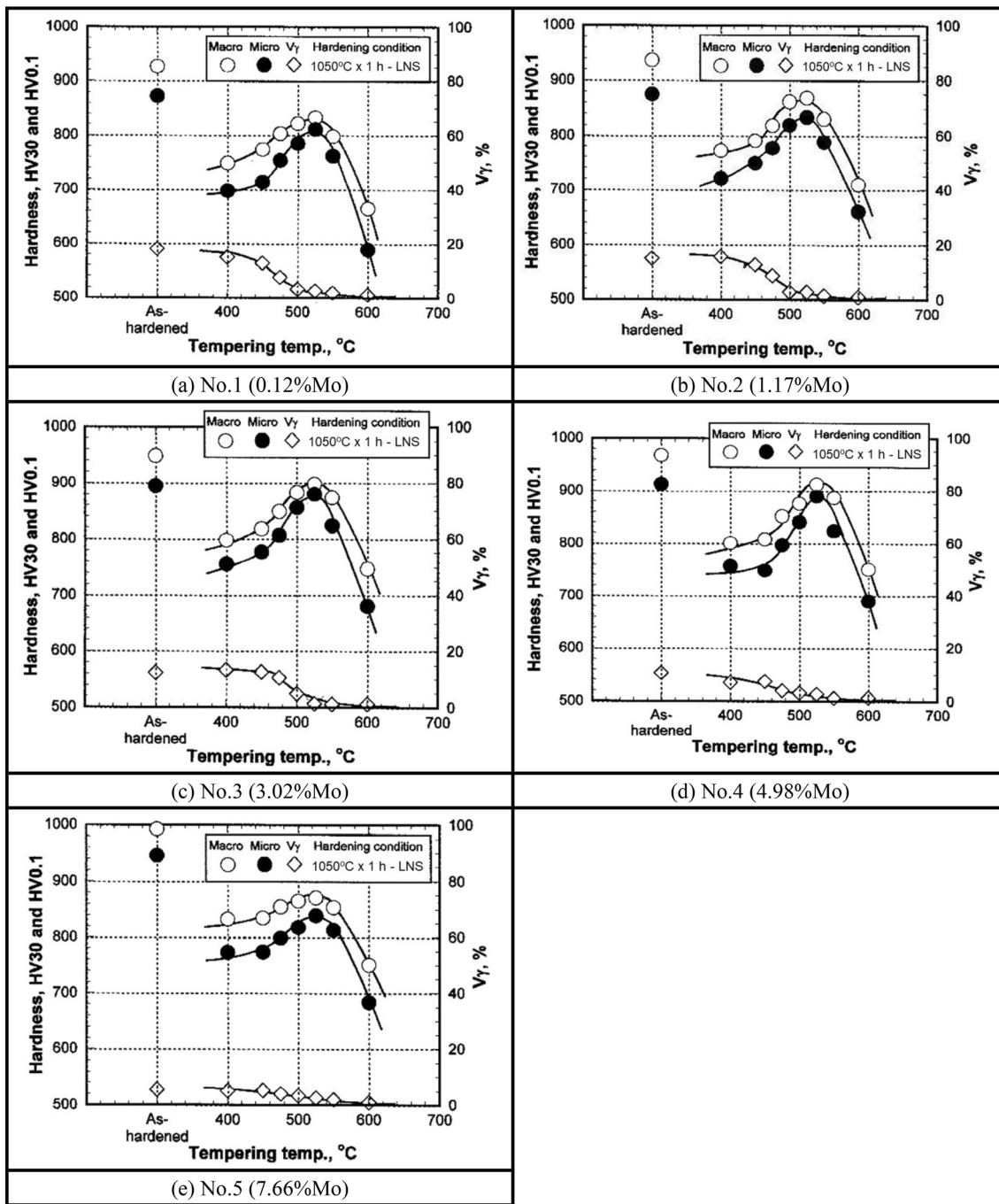
Figure 12. Relationship between macro-hardness, micro-hardness, volume fraction of retained austenite (Vγ) and tempering temperature of specimens with different Mo contents. Austenitizing: 1050 °C.

secondary hardening cannot take place in the over-tempering state.

In order to investigate the relationship between hardness and residual austenite in the tempered specimens, the macro-hardness and micro-hardness were connected to the Vγ values of all the tempered specimens and the relation is shown in Figure 14. Although the data were broadly scattered in a range of Vγ value less than 3%, the macro-

hardness and micro-hardness showed a similar trend in which the hardness increased to the maximum value and then, decreased as the Vγ value increased. It seems that a small amount of retained austenite did not affect the hardness. The decline in hardness over the maximum value was due to an increase in Vγ value which lowered the matrix hardness. The hardness over 850 HV30 which is necessary for the hot work roll was obtained within 5%Vγ.
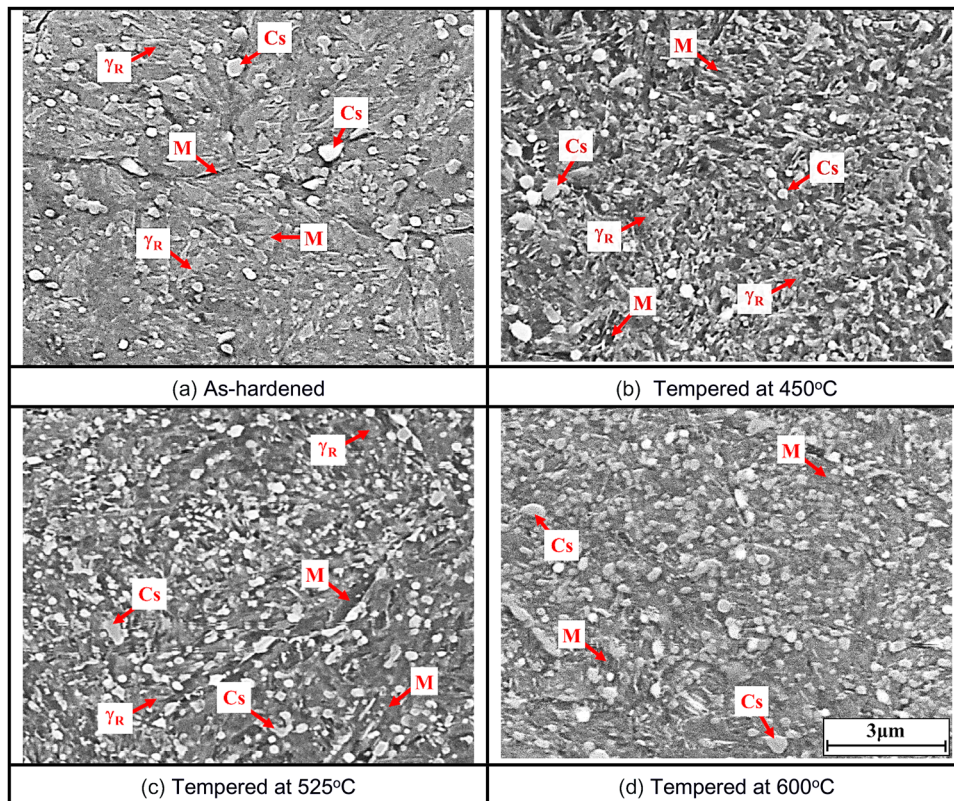
Figure 13. SEM microphotographs of specimens with 4.98%Mo tempered at different temperatures. Austenitizing: 1050 °C.
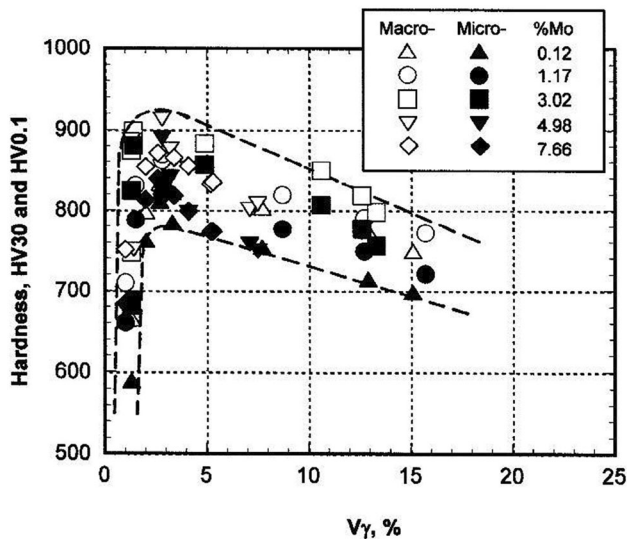

Figure 14. Relationship between macro-hardness, micro-hardness and volume fraction of retained austenite ($V\gamma$) in tempered specimens. Austenitizing: 1050 °C.

The maximum hardness values, 913 HV30 and 890 HV0.1, were obtained in the specimen with 4.98%Mo.

Since the tempering temperature does not vary the morphology of eutectic carbides, the scattering of hardness is mainly due to the difference in matrix structure or micro-
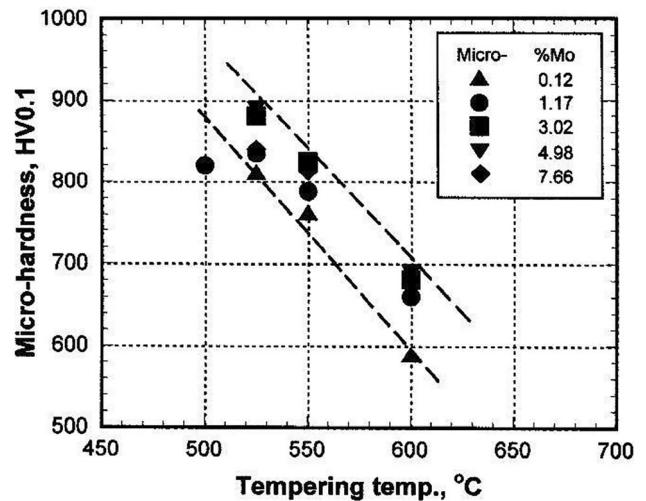

Figure 15. Relationship between micro-hardness and tempering temperature of specimens with $V\gamma$ values less than 3%. Austenitizing: 1050 °C.

hardness. For more comprehension, the relationship between micro-hardness and tempering temperature was made up for specimens with $V\gamma$ values less than 3% and is shown in Figure 15. The micro-hardness decreased clearly as the tempering temperature was elevated. It is presumed that the decrease in hardness was due to the coarsening of secondary carbide and the pearlitic or ferritic matrix.
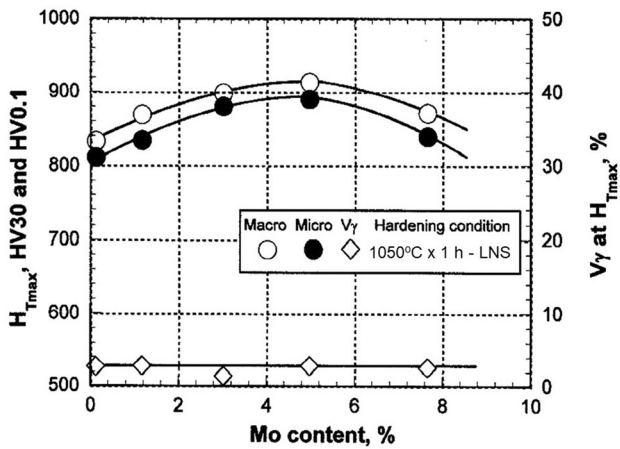
Figure 16. Effect of Mo content on maximum tempered hardness (H_{Tmax}) and volume fraction of retained austenite (V_γ) at H_{Tmax}.

Incidentally, the matrix in specimens tempered at 600°C was ferritic.

The effect of Mo content on the H_{Tmax} and $V\gamma$ value at H_{Tmax} is shown in Figure 16. The H_{Tmax} values of macro-hardness and micro-hardness varied similarly, corresponding to the Mo content. The H_{Tmax} increased to the highest value around 5% Mo and then, decreased. The $V\gamma$ value at the H_{Tmax} stabilized at about 3%. This suggests

that a certain amount of retained austenite still remained even in the H_{Tmax} specimen. To clarify how Mo affects the H_{Tmax} value, the SEM microphotographs of H_{Tmax} specimens with different Mo contents are representatively displayed in Figure 17. It is evident that the matrices in specimens consisted of secondary carbides (Cs), martensite (M) and retained austenite (γ_R). The size and amount of secondary carbides were different depending on the Mo content. The fine secondary carbides were observed in the specimens containing Mo less than 4.98% but the coarse secondary carbides were increased in the specimen with 7.66%Mo. It can be said that a low amount of Mo increased the number of secondary carbides but a high amount of Mo coarsens the secondary carbides.

It can be imagined that Mo promotes the formation of Mo carbide of M_2C or M_6C during heat treatment as well as other carbide formers of Cr, W and V, and they work on the improvement of secondary hardening. In the case of specimens with 7.66% Mo, however, the high hardness could not be obtained because of the large massed or coarse carbides produced by cohesion of fine carbides increased in number (Figure 17(d)). Moreover, a decrease in hardness of martensite itself which is caused by a lack of C in austenite just before martensite transformation could be another reason.
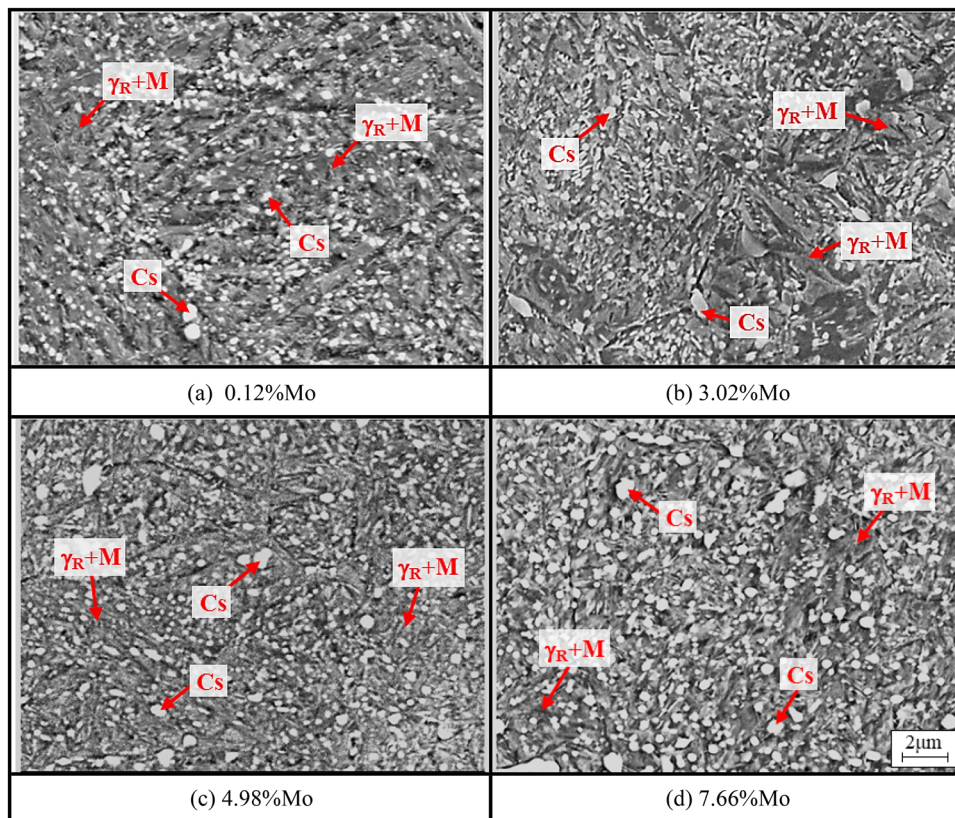
Figure 17. SEM microphotographs of H_{Tmax} specimens with different Mo contents. Austenitizing: 1050 °C.

From the above results, it can be seen that the highest value of H_{Tmax} was obtained in 4.98%Mo specimens and this result agrees with the previous work[12]. The highest value of H_{Tmax} in the previous work was 946 HV30, and it was only a little higher than that in this experiment. This can be explained by the fact that the higher austenitizing temperature produced a larger amount of retained austenite in the as-hardened state and caused more secondary hardening in the tempering. Consequently, a higher H_{Tmax} value was obtained. When the $V\gamma$ value at H_{Tmax} is compared, by contrast, the $V\gamma$ values of all specimens in this experiment were about 3%, and much lower than those in the previous work which varied from 3 to 10%.

It is known that the hardness demanded for hot working roll is more than 750 HV[2]. The H_{Tmax} values of all specimens in this experiment were higher than 750HV in the range of $V\gamma$ value less than 5%. As mentioned earlier for roll materials, the amount of retained austenite must be controlled to be as small as possible. Therefore, it can be said that the austenitizing at 1050 °C is not bad for heat treatment of roll materials to satisfy requirements such as hardness as well as a reasonable amount of retained austenite. However, it must be kept in mind that this kind of cast iron with heavy sections should be hardened at higher temperatures than 1050 °C for homogeneous austenitizing.

Conclusions

In this work, the effect of Mo content on solidification structure and heat treatment behavior of multi-alloyed white cast iron with Mo content from 0.12 to 7.66% was investigated. The solidification structures of the cast irons were verified by the thermal analysis techniques. For heat treatment, annealing, hardening from 1050 °C and tempering at 400–600 °C was applied to the cast irons. The results obtained can be summarized as follows:

1. The as-cast microstructure of all specimens consisted of primary austenite dendrite (γ_p) and eutectic structures (γ+carbide). The eutectics of (γ+MC) and (γ+M_7C_3) were observed in the specimens with Mo less than 1.17%. By contrast, the (γ+MC) and (γ+M_2C) eutectics were found in the specimens with Mo more than 3.02%.
2. According to the thermal analysis tests, solidification of specimens with Mo content of more than 3.02% began with γ_p, followed by the eutectic reactions of L→(γ+MC) and then, L→(γ+M_2C). The solidification temperature range of (γ+MC) eutectic decreased but that of (γ+M_2C) eutectic increased with an increase in the Mo content. The beginning temperature of (γ+M_2C) eutectic solidification increased as the Mo content rose.
3. The area fraction of γ_p changed little even if the Mo content was varied. However, the area fraction of (γ+MC) eutectic decreased while (γ+M_2C) eutectic increased with an increase in Mo content.
4. The matrix structures of all the as-hardened specimens were composed of martensite, secondary carbide and retained austenite. The size and the amount of precipitated secondary carbides increased as the Mo content increased.
5. The hardness in the as-hardened state rose proportionally to the Mo content due to an increase in the amount of (γ+M_2C) eutectic, precipitated carbides and martensite. In contrast, the volume fraction of retained austenite ($V\gamma$) values decreased continuously as the Mo content rose.
6. The tempered hardness curve showed the secondary hardening and its degree depended on the Mo content. The maximum tempered hardness (H_{Tmax}) was obtained by 525 °C tempering regardless of the Mo content. The $V\gamma$ value in each specimen tended to decrease as the tempering temperature increased. The $V\gamma$ value reduced greatly in the tempering between 450 and 525 °C and that at H_{Tmax} was less than 3% regardless of Mo content.
7. The H_{Tmax} value increased first and subsequently decreased with an increase in the Mo content. The highest H_{Tmax} values of 913 HV30 and 890 HV0.1 were obtained in the specimen with 4.98%Mo.
8. The austenitizing temperature of 1050 °C was suitable for heat treatment of roll materials to satisfy the hardness requirement for hot work roll with a reasonable amount of retained austenite.

REFERENCES

1. G. Laird, R. Gundlach, K. Rohrig, *Abrasion-Resistance Cast Iron Handbook* (American Foundry Society, USA, 2000)
2. M. Hashimoto, Abrasion Wear Resistant Alloyed White Cast Iron for Rolling and Pulverizing Mills, 1-23 (2008)
3. Y. Matsubara, N. Sasaguri, and M. Hashimoto, The 4th Asian Foundry Congress-Australia, 251-261 (1996).
4. I. Chakrabarty, Int. Metalcast. **5**, 49–56 (2011). https://doi.org/10.1007/BF03355507
5. Z. Özdemir, Int. Metalcast. **15**, 952–961 (2021). https://doi.org/10.1007/s40962-020-00532-0
6. S. Inthidech, P. Sricharoenchai, Y. Matsubara, Int. Metalcast. **6**, 25–34 (2012). https://doi.org/10.1007/BF03355536
7. Y. Sano, T. Hattori, M. Haga, ISIJ Int. **32**, 1194–1201 (1992). https://doi.org/10.2355/isijinternational.32.1194
8. M. Hashimoto, S. Otomo, K. Yoshida, K. Kimura, R. Kurahashi, T. Kawakami, T. Kouga, ISIJ Int. **32**, 1202–1210 (1992). https://doi.org/10.2355/isijinternational.32.1202
9. T. Kimura, M. Ishii, K. Amano, S. Ueda, Y. Oka, S. Nakano, ISIJ Int. **32**, 1224–1231 (1992). https://doi.org/10.2355/isijinternational.32.1224
10. M. Hashimoto, O. Kubo, Y. Matsubara, ISIJ Int. **44**, 372–380 (2004). https://doi.org/10.2355/isijinternational.44.372
11. H.Q. Wu, N. Sasaguri, Y. Matsubara, M. Hashimoto, AFS Trans. **104**, 103–108 (1996)
12. T. Meebupha, S. Inthidech, P. Sricharoenchai, Y. Matsubara, Mater. Trans. **58**, 655–662 (2017). https://doi.org/10.2320/matertrans.M2016396
13. W. Khanitnantharak, M. Hashimoto, K. Shimizu, K. Yamamoto, N. Sasaguri, Y. Matsubara, AFS Trans. **117**, 435–444 (2009)
14. J. Opapaiboon, M.S.N. Ayudhaya, P. Sricharoenchai, S. Inthidech, Y. Matsubara, Mater. Trans. **60**, 346–354 (2019). https://doi.org/10.2320/matertrans.M2018318
15. J. Opapaiboon, P. Sricharoenchai, S. Inthidech, Y. Matsubara, Mater. Trans. **56**, 720–725 (2015). https://doi.org/10.2320/matertrans.M2015001
16. S. Inthidech, K. Yamamoto, Y. Matsubara, Int. Metalcast. **15**, 229–240 (2021). https://doi.org/10.1007/s40962-020-00449-8
17. S. Inthidech, Y. Matsubara, Int. Metalcast. **14**, 132–143 (2020). https://doi.org/10.1007/s40962-019-00343-y
18. N. Sasaguri, K. Yamamoto, Y. Yokomizo, K. Shimizu, Y. Matsubara, J. JFS. **82**, 667–673 (2010). https://doi.org/10.11279/jfes.82.667
19. J. Opapaiboon, M.S.N. Ayudhaya, P. Sricharoenchai, S. Inthidech, Y. Matsubara, J. Met. Mater. Miner. **28**, 94-105 (2018) http://jmmm.material.chula.ac.th/index.php/jmmm/article/view/444
20. K. Chongmin, J. Heat Treat. **1**, 43–51 (1979). https://doi.org/10.1007/BF02833237
21. M. Hashimoto, O. Kubo, N. Sasaguri, Y. Matsubara, J. JFS. **76**, 205–211 (2004). https://doi.org/10.11279/jfes.76.205
22. G. Roberts, G. Krauss, and R. Kennedy, Tool Steels (ASM International, 2000)
23. K. Monma, Tekkouzairyougaku. Jikkyo shuppan, Tokyo, 1980